Geostatistical Mapping of Mountain Precipitation Incorporating Autosearched Effects of Terrain and Climatic Characteristics

HUADE GUAN AND JOHN L. WILSON

Department of Earth and Environmental Science, New Mexico Institute of Mining and Technology, Socorro, New Mexico

OLEG MAKHNIN

Department of Mathematics, New Mexico Institute of Mining and Technology, Socorro, New Mexico

(Manuscript received 20 December 2004, in final form 30 March 2005)

ABSTRACT

Hydrologic and ecologic studies in mountainous terrain are sensitive to the temporal and spatial distribution of precipitation. In this study a geostatistical model, Auto-Searched Orographic and Atmospheric Effects Detrended Kriging (ASOADeK), is introduced to map mountain precipitation using only precipitation gauge data. The ASOADeK model considers both precipitation spatial covariance and orographic and atmospheric effects in estimating precipitation distribution. The model employs gauge data and a multivariate linear regression approach to autosearch regional and local climatic settings (i.e., infer the spatial gradient in atmospheric moisture distribution and the effective moisture flux direction), and local orographic effects (the effective terrain elevation and aspect). The observed gauge precipitation data are then spatially detrended by the autosearched regression surface. The spatially detrended gauge data are further interpolated by ordinary kriging to generate a residual precipitation surface. The precipitation map is then constructed by adding the regression surface to the kriged residual surface. The ASOADeK model was applied to map monthly precipitation for a mountainous area in semiarid northern New Mexico. The effective moisture flux directions and spatial moisture trends identified by the optimal multiple linear regressions, using only gauge data, agree with the regional climate setting. When compared to a common precipitation mapping product [Precipitation-elevation Regression on Independent Slopes Model (PRISM)], the ASOADeK summer precipitation maps of the study area agree well with the PRISM estimates, and with higher spatial resolution. The ASOADeK winter maps improve upon PRISM estimates. ASOADeK gives better estimates than precipitation kriging and precipitation-elevation cokriging because it considers orographic and atmospheric effects more completely.

1. Introduction

Many hydrologic and ecologic studies recognize the importance of characterizing the temporal and spatial variability of precipitation (e.g., Goodrich et al. 1995; Bindlish and Barros 2000). This variability is even larger in mountainous regions because of complex topography and orographic effects (Barry 1992; Oki et al. 1991; Sturman and Wanner 2001; Sotillo et al. 2003). Orographic effects account for incoming moisture that is forced to rise by the topographic height, leading to more precipitation on the windward side, less precipitation on the leeward side, and more precipitation at higher elevations [cf. Barros and Lettenmaier (1993, 1994) and Michaud et al. (1995) for details on orographic mechanisms]. Because of orographic effects and other mesoscale climatic processes, the climate at high elevations is usually quite different from that at the low elevations, and thus is not captured by the gauges located at the lower elevations. A lack of adequate gauge stations at high elevations and precipitation in the form of snow—very common in mountainous regions during late fall, winter, and early spring—further complicate data collection and synthesis. Recently, radar has improved the estimation of spatially distributed precipitation; however, beam blockage, underestimation, and nondetection of precipitation are significant problems in mountainous terrains (Young et al. 1999). In addition, a reliable radar algo-

Corresponding author address: Huade Guan, Dept. of Earth and Environmental Science, New Mexico Institute of Mining and Technology, Leroy Place 801, Socorro, NM 87801.
E-mail: hdguan@nmt.edu

rithm for estimating precipitation as snow is not yet available. With their large topographic relief and gradient, and water storage as snow and ice, mountain hydrologic and ecologic systems are particularly sensitive to climate variability and change (Diaz et al. 2003; Beniston 2003).

Thus, a reliable precipitation mapping approach based on a limited number of gauge data is still desired for mountain areas. Various approaches have been applied to map precipitation from gauge observations. They include 1) those ignoring spatial covariance structure and knowledge of precipitation processes (such as orographic effects), for example, Theissen polygon and inverse square distance (reviewed by Goovaerts 2000); 2) those considering precipitation spatial covariance structures, for example, kriging (Phillips et al. 1992; Goovaerts 2000); 3) those considering orographic and/or atmospheric effects on precipitation occurrences, for example, regression (Daly et al. 1994; Michaud et al. 1995; Goovaerts 2000; Drogue et al. 2002); and 4) those considering both spatial covariance and terrain and/or climatic conditions, for example, cokriging precipitation with terrain elevation (Hevesi et al. 1992; Phillips et al. 1992; Goovaerts 2000) and detrended residual kriging (Phillips et al. 1992; Goovaerts 2000; Kyriakidis et al. 2001). Goovaerts (2000) compared seven techniques used to map monthly rainfall data for the Algarve region in Portugal and concluded that geostatistical kriging methods are better than traditional simple techniques (Theissen, inverse square distance, regression), and methods considering the secondary variables further improved the predictions. Terrain elevation is the most commonly used secondary variable incorporated in estimating precipitation, based on the physics of orographic effects. However, Goovaerts (2000) also found that the benefits of methods incorporating terrain elevation depend on the correlation coefficient between precipitation and elevation. The author proposed a threshold correlation coefficient of 0.75 for useful precipitation-elevation cokriging. Asli and Marcotte (1995) also reported that the introduction of secondary information in estimation is worthy only for correlation coefficient above 0.4. This would restrict the usefulness of the terrain elevation in cases where the correlation coefficient is low.

Terrain aspect, and its relationship to moisture sources, also play a role in orographic effects, and thus should be considered in precipitation estimates (Hutchinson 1973; Sturman and Wanner 2001; Sotillo et al. 2003). These effects increase the spatial variability of precipitation on complex terrains, which is not captured by low-spatial-resolution precipitation products. The Precipitation-elevation Regression on Independent Slopes Model (PRISM) provides an approach to couple both terrain elevation and aspect in estimating precipitation (Daly et al. 1994). In PRISM the terrain is divided into many topographic facets; in each facet the terrain aspect effect is assumed constant. A precipitation-elevation linear regression is constructed for each facet as the precipitation predictor for digital elevation model (DEM) grid cells in that topographic facet. As required for a reliable regression function, each topographic facet must be large enough to include a required number of gauge stations (although there are special algorithms to handle facets that cannot meet this requirement). By doing this, PRISM screens out the terrain aspect effects in its regression, which otherwise should be considered but are very often ignored in most other mapping approaches. More recently, PRISM uses weighting functions to incorporate gauge data of neighboring topographic facets for regressions, which involves a sophisticated parameterization (Daly et al. 2002). Sufficient regional climatic knowledge, which is not always available, is required for the PRISM weighting parameterization. In any event, the resolution of the PRISM product has been limited by its input DEM grid size ($\sim$6 km $\times$ 9 km) (Daly et al. 1994), although recently PRISM provides products with a resolution up to $\sim$2 km using a filtering algorithm. In other work, Basist et al. (1994) explicitly introduce elevation, slope (terrain steepness associated with the prevailing wind), orientation (relationship between the terrain aspect and the prevailing wind), and exposure (distance between the gauge and the mountain to the upwind direction of the gauge) into annual precipitation regressions. Similar to PRISM, their approach requires sufficient regional climatic knowledge and appears to apply for low spatial resolutions. Recently, Brown and Comrie (2002) used stepwise multiple linear regression for mapping winter temperature and precipitation in Arizona and New Mexico, with a spatial resolution of 1 km $\times$ 1 km. But the predictor variables are complex.

In this study, we use a multivariate linear regression approach conditioned on gauge data to autosearch regional and local climatic settings (i.e., infer the spatial gradient in atmospheric moisture distribution and the effective atmospheric moisture flux direction) and local orographic effects (the effective terrain elevation and the effective terrain aspect). The regression function captures the physical process effects leading to spatial variability of precipitation on complex terrain; thus, it should be useful for downscaling low-spatial-resolution precipitation products (not explored in this paper). The observed gauge precipitation data are then spatially detrended by the autosearched regression surface. The spatially detrended gauge data are further interpolated by ordinary kriging to generate a residual precipitation surface. The precipitation map is then constructed by adding the regression surface to the kriged residual surface. This approach is called Auto-searched Orographic and Atmospheric Effects Detrended Kriging (ASOADeK) (Figure 1). ASOADeK produces high-spatial-resolution precipitation maps explicitly incorporating terrain elevation and aspect, as well as climatic setting, while considering spatial correlation structure across the studied domain. In this paper, ASOADeK is compared to precipitation kriging, precipitation-elevation cokriging, and PRISM estimates for the long-term monthly average precipitation of a study area in northern New Mexico.

2. Methodology

a. Study area

The study area covers three National Climatic Data Center (NCDC) climate divisions (Fig. 2; DEM + weather stations) in northern New Mexico, with division 2 as the primary focus (Fig. 2a). Division 2 is mainly mountains (e.g., Sangre de Cristo Mountains) and intermountain valleys. The elevation ranges from 1290 to 3887 m according to the 1-km-resolution DEM map (Fig. 2b), which was resampled from a 60-m-resolution DEM (EDAC 1996). Altogether 74 NCDC weather stations that have at least 10-yr data available in the period of 1931–2003 and 9 snowpack telemetry (SNOTEL) stations with data available in the period of

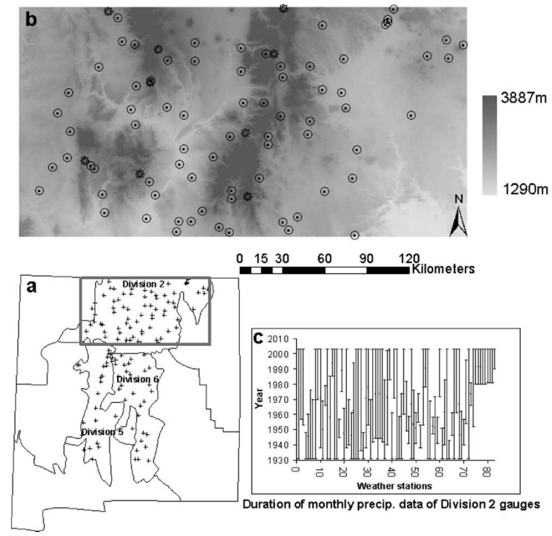

FIG. 2. Index map showing (a) the three climate divisions in New Mexico, (b) a division 2 DEM map with weather stations (asterisks are SNOTEL stations), and (c) the period of available data.

1980–2003 are used in this study. The SNOTEL system collects snowpack and related climatic data in the western United States. It is operated and maintained by the National Resource Conservation Service. The duration of the available data (NCDC and SNOTEL) is shown in Fig. 2c. Division 5 is the central valley along the Rio Grande rift, and division 6 is the central highlands. The mean annual precipitation, estimated as the averages of available long-term records, is 440, 240, and 410 mm for divisions 2, 5, and 6, respectively. We chose division 2 as the primary study area because it is mostly mountainous terrain, which is appropriate to test ASOADeK for mountain precipitation mapping.

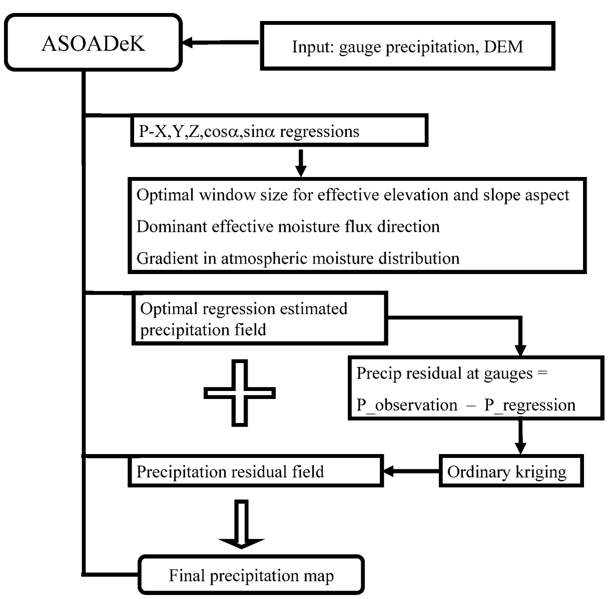

FIG. 1. Flow chart of the ASOADeK model.

b. Autosearching effective terrain and climatic characteristics

Because of orographic effects the long-term average precipitation (P) is usually well correlated with the terrain elevation (Z). However, it should be noted that due to complex climatic processes, such as channeling and convergence, simple positive P–Z correlation does not always hold. It has also been noticed in other studies that the optimal correlation elevation is not necessarily the point elevation, but more often is the effective elevation of a larger area (called the window) surrounding the observation point (Daly et al. 1994; Kyriakidis et al. 2001). The window usually has a square shape. In this study, the window for each gauge is located by comparing the gauge coordinate with the DEM maps of different pixel sizes generated by the ESRI (Redlands, California) ArcMap GIS tool.

Elevation is not the only orographic factor influencing precipitation; the terrain aspect may also play a role. Orographic effects depend on both terrain characteristics and the moisture flux direction (e.g., Oki et al. 1991; Sturman and Wanner 2001; Sotillo et al. 2003), the latter varying with season. It is difficult to distinguish terrain effects in annual precipitation because the effects of different seasons lump together and partially (or even completely) obscure these effects. Nonetheless, it is reasonable to assume that the mean moisture flux direction does not change much within a short period in the year (e.g., a month). In this short period, the moisture flux–related terrain aspect effects on precipitation should be detectable and can be used to improve precipitation estimates. In this event, just as effective elevation has an optimal window size, the terrain aspect must also have optimal window sizes demonstrating effective orographic effects. The optimal window size is determined from the best regression that has a minimum residual of the regression estimates with respect to the gauge observations.

Obviously, the availability of atmospheric moisture controls the precipitation distribution. If the moisture flux entering the study area is spatially inhomogeneous, so too will be the precipitation distribution transverse to the flow path. Our model simplifies this process, representing only a linear spatial gradient in moisture and precipitation (across the flow path). If, on the other hand, the atmospheric moisture depletes enough to cause different precipitation along the flow path, this also leads to a spatial gradient in precipitation distribution. We consider both of these processes together, although they can be separated using the inferred moisture flux direction (see section 4). In this paper, the atmospheric moisture gradient orientation is defined as 0° if it is wetter in the north, increasing clockwise, and 180° if it is wetter in the south. Like moisture flux direction, moisture gradient is inferred from the regression of gauge data, without reference to other data sources.

ASOADeK considers the terrain elevation, the relationship of moisture flux direction and terrain aspect, and the spatial gradient of moisture distribution as independent variables for precipitation estimates. In order for the effects of these variables to be automatically inferred through regression, they are explicitly introduced in the regression function (1). Above-sea-level terrain elevation (Z) in kilometers is used in this study. Since, the effect of terrain aspect (α) works together with moisture flux direction (ω), they are included to a cosine function, $\cos(\alpha - \omega)$. The aspect is defined as the direction of the slope orientation, 0° to the north, increasing clockwise, and 180° to the south; ω is the source direction of moisture flux, 0° from the north, increasing clockwise, and 180° from the south. The universal transverse mercator (UTM) easting (X) and northing (Y) of the precipitation gauges, with a unit of kilometers, are used to search the spatial gradient in atmospheric moisture:

$$P = b_0 + b_1X + b_2Y + b_3Z + b_4 \cos(\alpha - \omega). \quad (1)$$

Equation (1) can be further transformed to

$$P = b_0 + b_1X + b_2Y + b_3Z + b_5 \cos\alpha + b_6 \sin\alpha, \quad (2)$$

where $b_5 = b_4 \cos \omega$ and $b_6 = b_4 \sin \omega$ implicitly contain the moisture flux direction. With this equation, the elevation effect is autodetermined by b_3; the spatial gradient in atmospheric moisture is autodetermined by b_1 and b_2; and the moisture flux–dependent aspect effect is autodetermined by b_5 and b_6. The effective moisture flux direction itself can be retrieved from b_5 and b_6. For example, if b_5 and b_6 are both positive, $\omega = \mathrm{atan}(b_6/b_5)$. Similarly, the gradient in atmospheric moisture can be retrieved from b_1 and b_2. Five window sizes for terrain aspect and terrain elevation are considered for each month in the linear regression. The regression with the least mean absolute error (MAE) gives the optimal window sizes for orographic characteristics, and the effective dominant moisture flux direction, as well as the gradient in moisture distribution. The statistical significance of each variable in the regression is evaluated by analysis of the regression variance (ANOVA). These multiple linear regression procedures are the first components of ASOADeK model (Fig. 1).

c. *Precipitation mapping procedure*

1) CONSTRUCT THE OPTIMAL REGRESSION PRECIPITATION MAP

The regression precipitation map is constructed from the coefficients of the optimal regression function as determined in last section (i.e., known b_0, b_1, b_2, b_3, b_5, and b_6), and from the terrain elevations and aspects (i.e., X, Y, Z, α; all derived from a DEM) of the optimal window sizes. Since the optimal window size for the terrain elevation may be different from that for the terrain aspect, the regression precipitation map has a spatial resolution of the smaller window size. In this study long-term-average monthly precipitation maps were constructed. The optimal regression of significant terrain and climatic characteristics is our first-order estimate of monthly precipitation.

2) CONSTRUCT THE PRECIPITATION RESIDUAL MAP

From the optimal regression, and the determined effective orographic windows, the residual ($P_{\mathrm{observation}}$ −

$P_{\text{regression}}$) is calculated for each gauge. These precipitation residuals represent the spatial precipitation variability that is not covered by the deterministic relationship represented in the regression functions. The precipitation residual map can be constructed using ordinary kriging. In this study, Geostatistical Software Library (GSLIB) routines (Deutsch and Journel 1998) were used to calculate the experimental variograms of the precipitation residuals, and to construct the residual maps. The residuals are punctual at respective gauge locations and can be kriged to generate a residual map of any resolution. However, the information on the kriging map depends on the data availability. It is not necessary to use too high a resolution given the sparse gauges. Usually, the residual map has the same pixel size as the regression precipitation map. In geostatistics this procedure is called detrended kriging (also residual kriging) because the regression removes the trend attributed to the deterministic effects of climatic and orographic factors, leaving the residual as a near-random variable. Detrended kriging is the second component of the ASOADeK model. In this paper the variogram models were fitted to the calculated variograms manually (although this step can also be automated using, e.g., a maximum likelihood approach).

3) Construct the final precipitation map

The final monthly precipitation map is obtained by adding the kriged residual map and the regressed precipitation map (Fig. 1).

d. ASOADeK model testing

Other geostatistical approaches, such as ordinary kriging of observed precipitation and cokriging of precipitation with terrain elevation, are also applied to the same data and compared to ASOADeK estimates. The theory of kriging and cokriging of precipitation is well demonstrated in the literature (Hevesi et al. 1992; Goovaerts 2000; Kyriakidis et al. 2001) and is not described here. Cross validations are done to evaluate the performance of ASOADeK and other geostatistical approaches. "In cross validation actual data are dropped one at a time and re-estimated from some of the remaining neighboring data. Each datum is replaced in the data set once it has been re-estimated" (Deutsch and Journel 1998). For kriging and cokriging, cross validation is done in the kriging processes. For ASOADeK, cross validation is done from regression through kriging processes, with an assumption that the monthly variogram models do not change with one datum dropped out.

The PRISM monthly mean precipitation product is

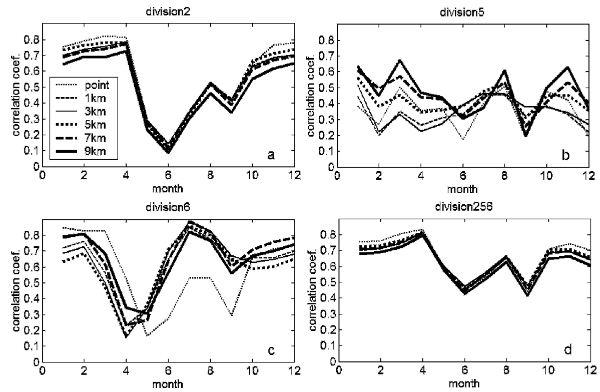

FIG. 3. Pearson correlation coefficient of mean monthly precipitation and the terrain elevation of various window sizes for NCDC New Mexico divisions (a) 2, (b) 5, and (c) 6 individually, and (d) lumped together (division 2 includes both NCDC and SNOTEL stations).

also compared to ASOADeK. The PRISM data are downloaded from Spatial Climate Analysis Service (2003). The PRISM data were estimated from the average monthly precipitation over 30 yr from 1971 to 2000, with a spatial resolution of about 4 km. PRISM is not included in the cross validation, as the necessary information to perform an equivalent and full cross validation is not available.

3. Results

a. Correlation of precipitation and terrain elevation

We calculated the Pearson correlation coefficients for mean monthly precipitation and elevation, using the point elevation for each gauge and the effective DEM elevations for five different window sizes around each gauge (Figure 3). The various-resolution DEM maps for the windows were derived from a 60-m DEM map using the ERDAS (Atlanta, Georgia) image-processing tool. The P–Z correlation is high in the winter months for the mountainous terrain of division 2. If we adopt a correlation coefficient of 0.75 as the threshold for meaningful cokriging P with Z, cokriging in division 2 should only be attempted for a few months. For the central highlands of division 6, the P–Z coefficient is high for all but April and May. The correlation is low for the central valley division 5, where the terrain is relatively flat. The best effective elevation windows, maximizing correlation, vary between months for divisions 5 and 6, while the effective elevation is not sensitive to the window size for division 2. Combining all three divisions compensates for opposing high and low correlations, losing information for geostatistical estimation. Cokriging P with Z, using the combined data of the three divisions, which has a combined P–Z relationship different from that for each division, would lead to biased estimates for precipitation.

b. *Regression of precipitation with terrain and climatic characteristics*

Since the effective elevation is not sensitive to window size in division 2, we used a 1-km DEM elevation window in the following regression analyses of division 2 precipitation gauge data. For more general situations, cross-combinations of different window sizes for elevation and terrain aspect should be tested. The tested regressions included precipitation–elevation (PZ: $P = b_0 + b_3 Z$), precipitation–elevation and aspect (PZA: $P = b_0 + b_3 Z + b_5 \cos \alpha + b_6 \sin \alpha$), precipitation-elevation, aspect, and spatial gradient of atmospheric moisture (PZAXY: $P = b_0 + b_1 X + b_2 Y + b_3 Z + b_5 \cos \alpha + b_6 \sin \alpha$). PZAXY is the ASOADeK regression of this paper. The results are shown in Fig. 4 and Tables 1 and 2, and are reported below. The general trend is that compared to the PZ regression, adding aspect improves the regression fitting and adding both terrain aspect and atmospheric moisture gradient further improves the regression fitting (Fig. 4). The relative importance of the three properties varies with months (Table 1; note the ANOVA F statistics). For winter months (November through April), both terrain elevation and aspect significantly influence the precipitation distribution. For summer monsoon months (July and August), elevation, terrain aspect, and the spatial gradient of atmospheric moisture all play a role in the precipitation distribution. For the first transition months (May and June), elevation is not an important factor for precipitation processes. For the second transition months (September and October), the elevation is the only factor significantly influencing precipitation distribution. The ASOADeK regression was examined for heteroskedasticity. Some heteroskedasticity was observed for winter months, suggesting nonlinear relationships between precipitation and the predictors for these months.

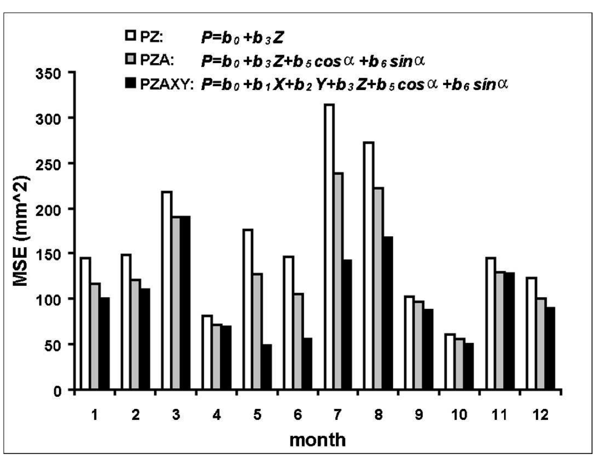

FIG. 4. Mean squared error of various precipitation (P) regression estimates for division 2.

TABLE 1. The R^2 values and F statistical test of ANOVA for significance of various orographic and atmospheric properties in precipitation regressions. For each regression type a boldface F statistic indicates that the variable or variables are significant for that month. Note that the data in the second column of each regression are ratios of mean of squares for regression due to the interested variables to mean squared error; $F^{0.005}$ is the critical threshold of 99.5% confidence level, above which adding the variable in regression is significant.

Regressions	PZ		PZA		PZAXY	
Month	R^2 (%)	Z	R^2 (%)	Aspect	R^2 (%)	X, Y
1	47	**72.39**	59	**11.25**	65	**7.36**
2	53	**90.67**	63	**10.41**	67	4.75
3	55	**99.06**	62	**6.87**	63	1.15
4	60	**119.68**	65	**6.29**	67	2.42
5	8	7.43	36	**16.67**	76	**62.87**
6	2	1.74	31	**16.39**	65	**37.25**
7	11	**10.22**	34	**13.74**	62	**27.79**
8	27	**30.43**	42	**10.30**	58	**13.76**
9	18	**18.13**	25	3.28	34	5.30
10	40	**54.55**	48	5.51	53	4.87
11	47	**71.53**	54	**6.16**	55	1.19
12	49	**78.14**	60	**10.26**	65	**5.79**
$F^{0.005}$		8.33		5.67		5.68

The optimal window size for effective terrain aspect in PZAXY regression varies from 3 to 9 km, depending on the month, but is mostly around 5 km (Table 2). This is much smaller than the topographic facet used in PRISM (Daly et al. 1994). The effective moisture flux direction, retrieved from PZAXY regressions, varies with time, from southwesterly and southerly in winter, transitioning to southeasterly and southerly in summer (column 3 in Table 2). The regression identified atmospheric moisture gradient also varies with month, suggesting different atmospheric moisture characteristics in the study area through the year. Also note that the wetter direction is not necessarily upwind (see section 4).

ASOADeK regression results for three selected months (February, May, and August) are shown in Figure 5, with comparison to PRISM estimates. Of the three months, February represents the winter season, August is in the summer monsoon season, and May is a transition month in between and has weak elevation-correlated monthly precipitation. Even without the next step of detrend kriging of the residual, the

TABLE 2. The parameter values of the optimal linear regressions of monthly precipitation from ASOADeK for division 2 ($P = b_0 + b_1 X + b_2 Y + b_3 Z + b_5 \cos \alpha + b_6 \sin \alpha$).

Month	Aspect window	Moisture flux direction*	Moisture gradient**	b_0	b_1	b_2	b_3	b_5	b_6	MAE	MAE/P (%)	Mean precipitation (mm)
1	9 km	213	298	−145.73	−0.062	0.033	27.631	−6.093	−4.009	6.71	29	23.48
2	5 km	198	295	−137.11	−0.058	0.027	33.423	−6.789	−2.188	7.13	31	23.08
3	5 km	186	279	−80.43	−0.037	0.006	43.788	−9.095	−0.942	9.22	29	31.42
4	5 km	180	60	−136.44	0.035	0.020	29.854	−5.361	−0.018	5.90	20	29.52
5	3 km	174	86	−93.82	0.144	0.009	13.830	−5.150	0.516	5.37	14	38.54
6	3 km	136	121	247.94	0.122	−0.073	9.995	−2.297	2.223	5.70	17	32.97
7	3 km	156	134	542.10	0.155	−0.151	26.007	−7.683	3.499	8.92	14	64.91
8	9 km	172	145	513.29	0.100	−0.142	35.505	−11.946	1.624	10.38	14	74.59
9	5 km	172	154	272.15	0.035	−0.071	16.714	−5.138	0.686	7.06	17	42.60
10	5 km	182	195	181.05	−0.012	−0.047	19.227	−4.427	−0.147	5.43	16	33.94
11	5 km	180	281	−58.72	−0.047	0.009	29.527	−5.487	−0.016	7.77	31	25.46
12	5 km	191	273	−29.08	−0.062	0.003	28.428	−5.369	−1.046	6.37	28	22.51

* The incoming direction of the moisture flux, 0° from the north, increasing clockwise, and 180° from the south.

** The upgradient direction of the moisture spatial gradient, 0° from the north (i.e., wetter in the north), increasing clockwise, and 180° from the south.

ASOADeK regression shows estimating capacity close to that of PRISM, especially for May.

c. *ASOADeK precipitation maps*

At each gauge location, the detrended residual was calculated by subtracting the regression value from the gauge measurement. The semivariograms were constructed for the residuals and fit with standard models (Figure 6) and were used to perform residual kriging. Adding kriged maps of the detrended residual to the regression maps leads to the final ASOADeK precipitation maps. Final ASOADeK maps for each of three selected months are compared to PRISM precipitation maps in Figure 7. The spatial patterns of precipitation maps from the two approaches agree well. Regarding the estimated precipitation values, ASOADeK estimates for August are consistent with PRISM. For February, ASOADeK gives lower precipitation estimates at the locations with large PRISM precipitation rates. For May, ASOADeK consistently underestimates precipitation compared to PRISM. We also constructed the annual precipitation map by summing all 12-month precipitation maps (not shown). The mean annual precipitation for division 2 from the ASOADeK map is ~445 mm (the PRISM map ~460 mm), in good agreement with the arithmetic average of all observations (NCDC + SNOTEL) in the division (440 mm). This suggests that for division 2, the distribution of current gauges (including both SNOTEL and NCDC stations) captures the influence of topography on mean precipitation in the division. However, the mean of only the NCDC stations, 410 mm, significantly underestimates it. One advantage of the ASOADeK (and other kriging-based approaches) is that it can be used to estimate map uncertainty. They are calculated as the sum of regression variance and the kriging variance. The squared roots of the total variance for the three subject months are shown in Figs. 7a–c.

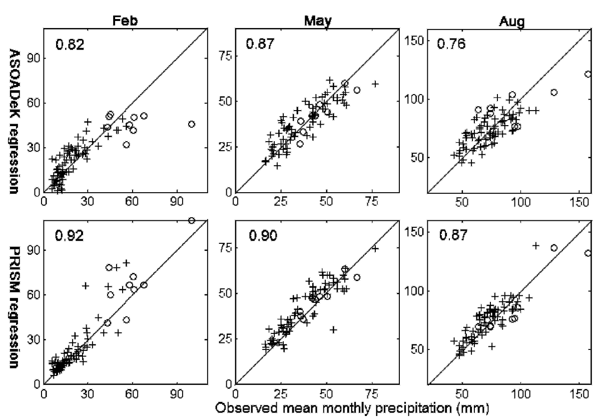

FIG. 5. Comparison of (top) ASOADeK ($PZAXY$) regression estimates to (bottom) PRISM estimates for three selected months in division 2. The x axis is the observed mean monthly precipitation, and y axis is model estimates. Cross legends represent NCDC stations, and circles represent the SNOTEL stations. The number inside each panel is the correlation coefficient between the estimates and the observations.

d. *Cross validation*

Since all gauge data have been used in the regressions, a good fit to the data does not necessarily indicate a good predicting capacity. In addition, the comparison

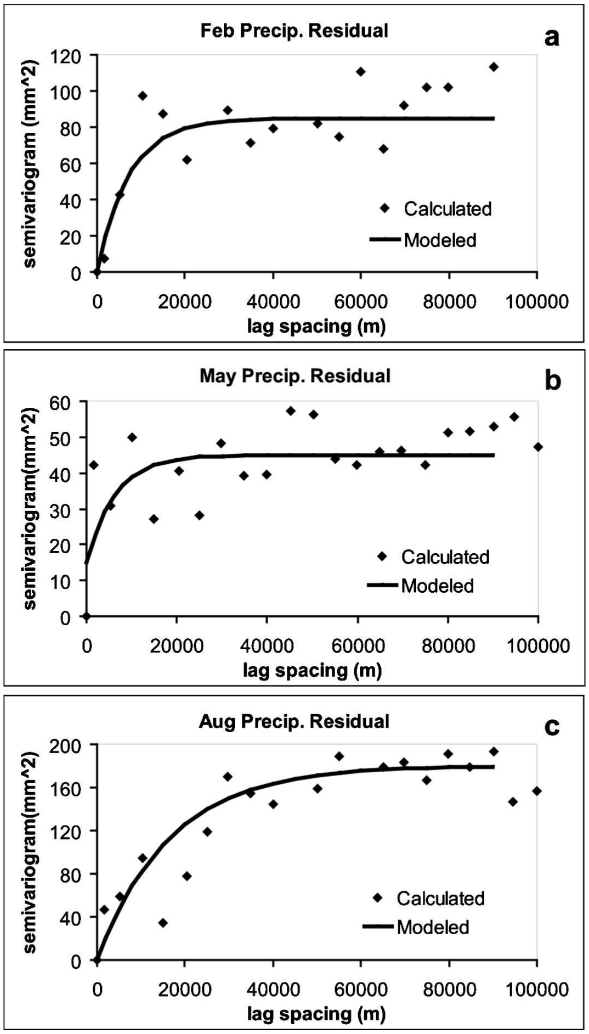

FIG. 6. Semivariograms of precipitation residuals for three selected months: (a) Feb, (b) May, and (c) Aug. Note that zero nuggets for some months (Feb and Aug) are a consequence of the semivariogram fitting method, not necessarily representing zero measurement error.

of the kriging estimates with the observed data used for kriging does not tell how good the estimates are. An extreme example is that zero-nugget semivariogram models would exactly give the observation values. Cross validations were thus conducted for various precipitation estimators, with results shown in Figs. 8 and 9 for three months (February, May, and August). It is not possible with available information to perform cross validations for PRISM in this study. For ASOADeK and other precipitation estimators (*P* kriging, *P–Z* cokriging, PZ regression, ASOADeK regression-only) tested in this study, the performance varies between months. For February and May, the ASOADeK regression works better than the precipitation kriging, *P–Z* cokriging, and PZ regression (Fig. 9 only). For August, the ASOADeK regression is better than PZ regression (Fig. 9 only), but poorer than *P* kriging and *P–Z* cokriging. For May, which has a weak *P–Z* correlation, precipitation kriging gives better estimates than *P–Z* cokriging, which is consistent with other studies (Goovaerts 2000). For all months, ASOADeK estimates, which include both the ASOADeK regression and the kriged residual, are best.

4. Discussion

a. ASOADeK autosearching regional climate setting and local orographic effects

Long-term average precipitation is controlled by the regional climate setting and local conditions. In mountain regions, orographic effects have the strongest influence on precipitation distribution, as once again demonstrated in our study area (Table 1). Most precipitation mapping approaches only consider terrain elevation, which alone is not sufficient to represent the orographic effects. In our study area (division 2), *P–Z* correlation is very low for May and June, and low for monsoon months (Fig. 3), indicating elevation is not the dominant orographic factor for these months. In addition to elevation, ASOADeK explicitly introduces terrain aspect, moisture flux direction, and the atmospheric moisture gradient into the multivariate linear regression of gauge data, autosearching effective orographic and atmospheric characteristics for precipitation mapping, including effective orographic window sizes. These considerations significantly improve the precipitation estimates (Table 1; Fig. 4).

How well does the ASOADeK-identified moisture flux direction match the local climate setting? Two seasons typify the climate in the study area: the summer monsoon and winter storms. Although there is no settled scientific opinion about the moisture source of the North American monsoon (reviewed by Sheppard et al. 2002), it is agreed that the moisture (either from the Gulf of California or the Gulf of Mexico) for monsoon precipitation in the southwestern United States is developed over Mexico (e.g., Carleton 1986; Fawcett et al. 2002; Bosilovich et al. 2003). In other words, in summer monsoon months, the dominant moisture flux in the northern New Mexico study area is southwesterly. Monsoon precipitation is joined by local recycling of moisture as an additional source (Bosilovich et al. 2003). There are also occasionally nonmonsoonal summer precipitation events. Some of these events are caused by easterly atmospheric moisture flux (NOAA 2004). The effective moisture flux directions, determined by ASOADeK (Table 2; see PZA columns in

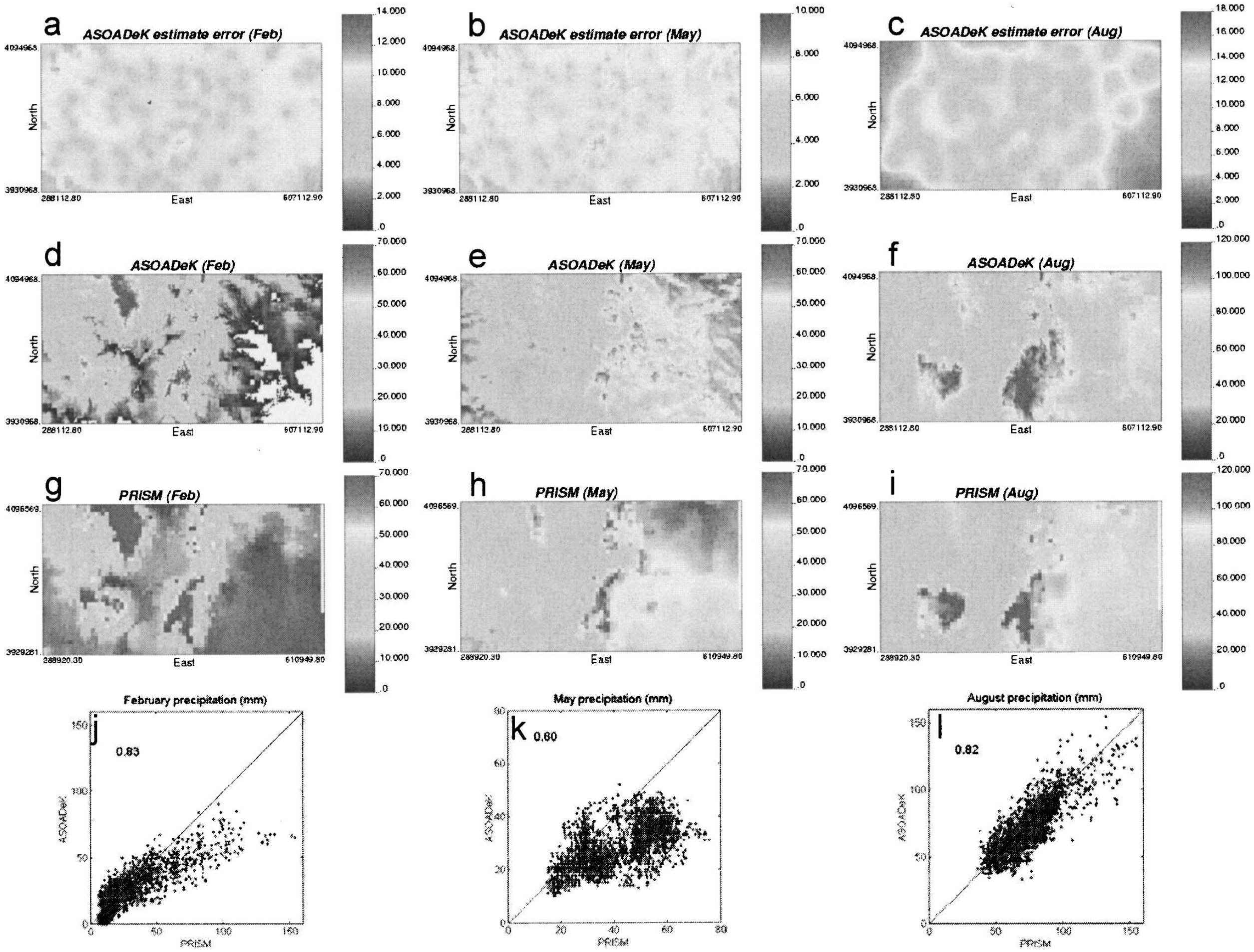

FIG. 7. (second row) ASOADeK-constructed mean monthly precipitation maps (mm) of division 2, with a spatial resolution of 1 km. (top row) The respective estimate error (square root of the sum of regression variance and kriging variance) maps. (third row) The PRISM estimates with a spatial resolution of ~4 km. (bottom row) The scatterplots between the ASOADeK products and resampled PRISM products. (a), (d), (g), (j) Feb; (b), (e), (h), (k) May; (c), (f), (i), (l) Aug. The number listed on the scatterplot is Pearson correlation coefficient of the two estimates. Since kriging variance contributes most of the total uncertainty, the ASOADeK estimate error inherits the pattern of the kriging variance. The smallest errors occur at the gauge locations, with a smaller propagation radius in May due to smaller range, and a bigger radius and range in Aug (Fig. 6).

Table 1 for significance), are SSE and S, for July and August, respectively, which is apparently the mixture of the southwesterly and easterly moisture fluxes. For winter months, most of time, Pacific moisture enters North America at latitudes well north of the study area, leading to dry weather in this area (Sheppard et al. 2002). "More favorable conditions for winter precipitation in the Southwest exist when the Pacific high shifts westward and a low pressure trough forms over the western United States, allowing Pacific storms to enter the continent at lower latitudes . . ." (Woodhouse and Meko 1997). Thus, the dominant moisture flux of winter months at the study area is southwesterly (Sellers and Hill 1974). This is more or less captured by ASOADeK, which infers southwesterly to southerly moisture flux direction for the winter months (Table 2).

Now, let us look at the spatial gradient of atmospheric moisture in the study area. If the moisture flux homogeneously enters the whole study area, the only gradient would be due to depletion of atmospheric moisture. The direction of the spatial gradient caused by depleted atmospheric moisture would then agree with flux direction, that is, more precipitation in the upwind direction of incoming moisture flux. A significant atmospheric moisture gradient that is in disagreement with the effective moisture flux direction suggests either that the entering moisture flux only covers a part of the study area or that there are two or more dominant moisture fluxes in the month. The ANOVA

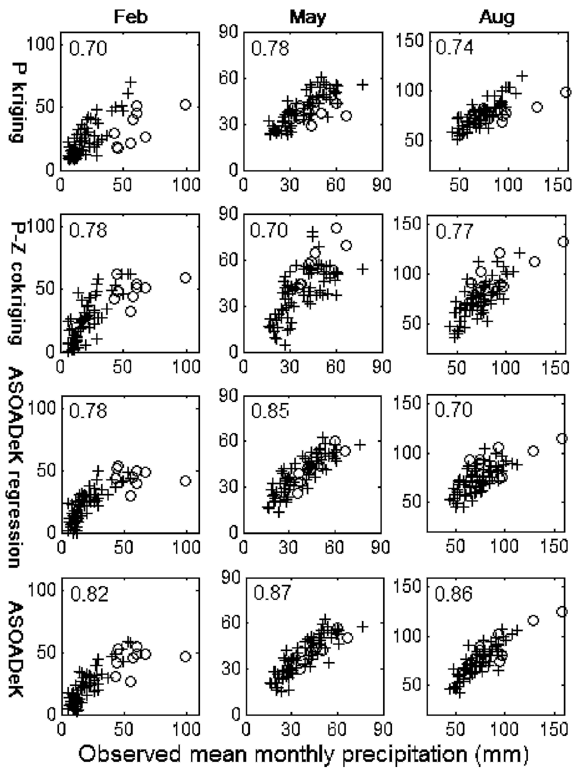

FIG. 8. Cross validation of precipitation kriging, *P–Z* cokriging, ASOADeK (PZAXY) regression, and ASOADeK estimates for three selected months, representing different seasonal climates. The *x* axis is the observed mean monthly precipitation, and the *y* axis is model estimates. Cross legends represent NCDC stations, and circles represent SNOTEL stations, for division 2. The number inside each panel is the correlation coefficient between estimates and the observations.

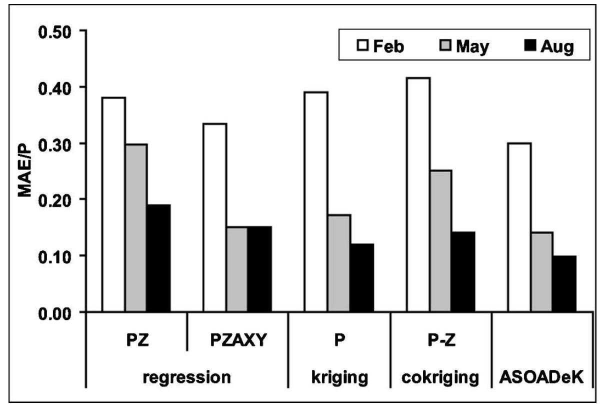

FIG. 9. Normalized mean absolute error of cross validations for various precipitation estimators in division 2.

analyses of ASOADeK regressions suggest that atmospheric moisture gradient is not important for most winter months and is only slightly significant for December and January (Table 1). In these months, the ASOADeK-determined spatial moisture gradient is from the west to the east (drier in the east), almost orthogonal to the monthly effective moisture flux direction also determined by ASOADeK (Table 2). Whether or not this represents an actual physical process requires further study. For the monsoon months, the moisture spatial gradient is close to the effective moisture flux direction, but still deviates by about 20° (Table 2). This is because there are two circulation patterns that bring moisture for showers and thunderstorms over New Mexico (NOAA 2004). For the premonsoon months (May and June), the moisture spatial gradient is the most significant factor influencing the monthly precipitation distribution in the study area (Table 1). In May, the moisture spatial gradient from ASOADeK is orthogonal to the effective moisture flux direction (Table 2). This is because in late spring, a northward low-level moisture flux migrates into the central United States from the Gulf of Mexico, causing a westward decreasing trend in May precipitation throughout the central and western United States (Mock 1996; Higgins et al. 1996, 1997). This low-level moisture flux touches the eastern edge of the study area, leading to an eastward moisture gradient (Table 2). ASOADeK successfully captures this climate pattern, and at the same time detects the southerly effective moisture flux direction as well. This northward movement of moisture provides a source for precipitation in the study area, indicated by the higher monthly precipitation in May than in April and June. It appears from this discussion that, in sufficiently mountainous terrain, and using gauge data alone, the ASOADeK algorithm can be used to infer the effective moisture flux direction and the spatial gradient of atmospheric moisture where the regional climate setting is otherwise unclear.

From the ANOVA analysis (Table 1), orographic effects of both terrain elevation and terrain aspect are significant for precipitation during winter and monsoon months. In the transition months, only one factor, either elevation or terrain aspect, plays a significant role. More work is required to reveal whether this is the result of different precipitation processes.

b. ASOADeK versus PRISM

Both ASOADeK and PRISM consider terrain aspect in precipitation estimation, but in different ways. In early versions of PRISM the terrain aspect effect is screened out in each topographic facet (Daly et al. 1994). In more recent versions, the aspect effect is described by a weighting function for *P–Z* regression (Daly et al. 2002). The physical mechanism is not well represented. To determine an appropriate weighting function, sufficient knowledge of regional and local climate is needed. In ASOADeK, the terrain aspect effect is explicitly associated with the effective dominant moisture flux direction, well representing the physical mechanism. The moisture flux–dependent aspect effect is also autodetermined in ASOADeK regression without background climate knowledge. Both ASOADeK and PRISM consider the spatial gradient of atmospheric moisture in estimating precipitation distribution. In PRISM, this is achieved by a weighting function in the *P–Z* regression based on distance to the moisture source (Daly et al. 2002). The distance to the moisture source is ambiguous because the moisture flow path is often tortuous. In addition, for a study area far away from the ocean, the effect of this variable becomes numerically negligible. In ASOADeK, the moisture gradient is automatically searched in high spatial resolution. This allows ASOADeK to represent the actual atmospheric spatial moisture trend in the area of interest, rather than tie it to a distant ultimate source of moisture. Regarding spatial resolution, PRISM depends on input DEM resolutions, currently about 4 km, while ASOADeK depends on the minimum of optimal window sizes for various orographic variables from the multivariate regressions. When effective elevation window size is nonsensitive to *P–Z* correlation, such as division 2 in this study, high-spatial-resolution precipitation maps can be obtained by prescribing a small window size for the effective terrain elevations used in the ASOADeK model. Regarding the mapping area, PRISM has been used to estimate precipitation in most areas of northern America, and for all topography types. The current version ASOADeK, however, is used to estimate precipitation for a mountainous area with more or less spatially consistent regional climate settings.

Of the three focused study months, the scatterplots (Figs. 7j–l) show that the ASOADeK monthly precipitation estimates agree well with PRISM for August. However, the February and May estimates for the two models differ. This suggests that either ASOADeK underestimates, or PRISM overestimates, precipitation for these months, or both. Let us focus on May first. That PRISM appears to slightly overestimate most of the May precipitation is clearly observed in Fig. 5. The fairly good cross validation of ASOADeK May precipitation (Fig. 8) also suggests that the difference between the two model estimates for May precipitation is due to PRISM overestimates. The ANOVA analysis of ASOADeK regression indicates that atmospheric moisture gradient and terrain aspect are two major physical factors for May precipitation distribution. Terrain elevation is not a significant predictor of precipitation in this month (Table 1). This makes the PRISM model (precipitation elevation regression) problematic for this month. In addition, the window size of effective terrain aspect, inferred from ASOADeK regression, is 3 km for May (Table 2), far smaller than the topographic facet of the PRISM model. Let us compare to August, for which PRISM and ASOADeK are in good agreement. The August *P–Z* correlation is significant (Fig. 3), and the effective terrain window size (9 km) is large (Table 2), apparently contributing to the good agreement between the two models.

Does PRISM also overestimate February precipitation? To answer this question, we have to exclude some other causes for the apparent PRISM overestimates of February precipitation shown in Figs. 5 and 7. First, the apparent overestimates could be because the time periods of observation data for PRISM estimates and those for the estimates in this study are not identical. Both PRISM and our estimates are based on long-term average, that is, 30 yr for PRISM from 1971 through 2000 and 11–73 yr for our estimates between 1931 and 2003. Comparison of the long-term averages of 1971–2000 to those of available records in the whole time range does show some difference, but not big enough to explain the apparent PRISM overestimates for February shown in Fig. 5. Besides, some PRISM overestimates happen at weather stations where both methods share almost the same data period of 1971–2003. Second, the apparent PRISM overestimates may be an artifact of the dataset's elevation range. The elevation of weather stations (1694∼3389 m) does not cover the full elevation range of the study area (1290–3887 m), especially with about 500 m of the higher-end elevation range missing any weather stations. Orographic effects at the high elevations probably deviate from those estimated from the lower elevations. PRISM applies a prescribed universal *P–Z* regression function for the high elevations where observations are lacking, while no adjustments have been done in ASOADeK. This could explain the difference between PRISM and ASOADeK in Fig. 7, but does not tell which gives better February estimates. The prescribed *P–Z* function in PRISM is not derived locally and may not represent the situation for our study area.

That ASOADeK underestimates higher February monthly precipitation values is observed in Fig. 8, but the underestimates are all at SNOTEL sites. The location with the most severe ASOADeK underestimate is SNOTEL site Hopewell. This site has a point elevation of 3048 m, but has a larger monthly precipitation rate for winter months than a higher 3389-m-elevation SNOTEL site, Wesner Spring. Hopewell is an outlier site that is not explained by our modeled orographic effects, or represented by other geostatistical approaches (Fig. 8). If this outlier is excluded, ASOADeK estimates look much better for this and other winter months. PRISM, however, predicts the precipitation at this location well, but overestimates at quite a few other locations (Fig. 5). We suggest that the apparent winter PRISM overestimates at these locations—winter here is not just February, for they occur from November through March (not shown)—are due to the nonlocal vertical extrapolation adjustment. This adjustment in PRISM is better for the monsoon months, as shown in Fig. 5 and in the scatterplot for August (Fig. 7).

Even removing the outlier in Fig. 8, we cannot exclude that ASOADeK underestimates monthly precipitation at some locations. Besides the outlier, the cross-validation results suggest that ASOADeK still slightly underestimates at a couple of observations for February, and one for August (Fig. 8). The linear regression employed in ASOADeK may not capture the precipitation distributions of the whole elevation range and could be improved by using nonlinear regressions. Of course, the above analysis is based on an assumption that the gauge data (both NCDC weather stations and SNOTEL stations) give unbiased measurement of precipitation amount.

c. ASOADeK versus other geostatistical approaches

Precipitation kriging only considers spatial covariance structure of the precipitation distribution; it does not capture the orographic effects. For February when *P–Z* correlation is high, precipitation kriging gives poor estimates (Figs. 8 and 9), while for May and August, when *P–Z* correlation is low, precipitation kriging gives fair estimates (Figs. 8 and 9). The *P–Z* cokriging considers both precipitation spatial covariance structures and partial orographic effects and is often used to map mountainous precipitation (e.g., Hevesi et al. 1992; Goovaerts 2000). However, cokriging requires high *P–Z* correlation, and the mathematical procedure for cokriging is more complex. For May with a low *P–Z* correlation, *P–Z* cokriging gives poor estimates (Figs. 8 and 9). Comparing MAE of precipitation kriging and *P–Z* cokriging, cokriging gives poorer estimates than kriging for all three closely studied months (Fig. 9). This supports the 0.75 threshold of *P–Z* correlation coefficient for useful cokriging, such as suggested by Goovaerts (2000). For annual average precipitation in which the different terrain aspect effects of the various months are compensated for via trade-off, *P–Z* cokriging may become a good tool for precipitation mapping in the mountainous regions (e.g., Hevesi et al. 1992). For February and May, ASOADeK regressions (i.e., without kriged residuals) give better estimates than kriging and cokriging, while for August, ASOADeK regression (PZAXY) does not outcompete precipitation kriging and *P–Z* cokriging estimates (Figs. 8 and 9). This is probably because summer storms occur more randomly in space with more local moisture recycling, and are more difficult for the regressions to capture. Adding its second component (i.e., detrended kriging of residuals), ASOADeK gives better precipitation estimates than precipitation kriging and cokriging for all months (Figs. 8 and 9). This is reasonable because kriging considers only the spatial covariance structures of the precipitation gauge data, while ASOADeK considers both the covariance information and the physical processes that influence precipitation distribution. Although *P–Z* cokriging incorporates the secondary information in addition to the spatial covariance of the precipitation gauge data, it does not include all the orographic and atmospheric effects on the precipitation distribution that are embedded in the ASOADeK model. Theoretically, all these orographic and atmospheric effects can also be included in cokriging with more secondary variables. But this is mathematically tedious and is limited by the currently available computational codes.

5. Conclusions

The purpose of this study is to introduce a geostatistical method (ASOADeK) to map mountain precipitation using only gauge data, while considering both precipitation spatial covariance structure and orographic and atmospheric effects. Application of ASOADeK to monthly precipitation in a mountainous area of northern New Mexico appears to outperform traditional kriging and cokriging approaches and produce a precipitation map comparable to the PRISM product, but with a higher spatial resolution. In contrast to PRISM, a knowledge-based approach, ASOADeK does not require detailed understanding of the regional climatic setting. Instead, it automatically detects orographic factors and the climate setting of the study area, including the spatial gradient of atmospheric moisture and the dominant moisture flux direction.

For the study area in northern New Mexico, ASOADeK successfully captures monthly moisture flux directions over the year, and the spatial moisture gradient for monsoon and premonsoon months. ASOADeK also suggests that the significance of orographic effects varies between months. For winter months, the terrain elevation is the primary factor, and the terrain aspect is the secondary factor. For monsoon months, both terrain elevation and aspect have similar impacts on precipitation distribution. However, only terrain aspect is important for May and June, and only terrain elevation is important for September and October. Further studies are required to reveal whether or not this is related to different precipitation processes between the months. If this is the case, it would suggest that ASOADeK has the capacity not only to map mountainous precipitation, but also to work as a diagnostic tool to help understand meteorological processes. In this sense, ASOADeK appears to use mountainous terrain as an instrument to detect or diagnose climate and weather patterns.

To further test the model, future work will include applications of ASOADeK to other mountain areas and to higher temporal resolutions (e.g., monthly precipitation of a specific year). With its capacity to map high-spatial-resolution precipitation, ASOADeK could be used to study climate variability (e.g., teleconnections with the Pacific decadal oscillation and the El Niño–Southern Oscillation) and its effects on mountainous precipitation distribution. With its autosearch capacity, ASOADeK regression has potential for recovering missed rainfall data in the Next-Generation Weather Radar (NEXRAD) shadow due to the mountain blockage, and for downscaling low-spatial-resolution precipitation products. It also has potential as a tool to help identify atmospheric moisture sources (e.g., moisture source of the North American monsoon).

Acknowledgments. Sean McKenna and Hongjie Xie assisted in preparing the manuscript. Valuable comments from David Gochis, Pierre Goovaerts, David S. Gutzler, Enrique R. Vivoni, Jianjun Xu, and Scot Johnson, and three anonymous reviewers are appreciated. This work was supported by the Sustainability of Semi-Arid Hydrology and Riparian Areas (SAHRA) under the STC Program of the National Science Foundation, Agreement EAR-9876800.

REFERENCES

Asli, M., and D. Marcotte, 1995: Comparison of approaches to spatial estimation in a bivariate contest. *Math. Geol.,* **27,** 641–658.

Barros, A. P., and D. P. Lettenmaier, 1993: Dynamic modeling of the spatial distribution of precipitation in remote mountainous area. *Mon. Wea. Rev.,* **121,** 1195–1214.

——, and ——, 1994: Dynamic modeling of orographically induced precipitation. *Rev. Geophys.,* **32,** 265–284.

Barry, R. G., 1992: Mountain climatology and past and potential future climatic changes in mountain regions. *Mt. Res. Dev.,* **12,** 71–86.

Basist, A., G. D. Bell, and V. Meentemeyer, 1994: Statistical relationships between topography and precipitation patterns. *J. Climate,* **7,** 1305–1315.

Beniston, M., 2003: Climatic change in mountain regions: A review of possible impacts. *Climatic Change,* **59,** 5–31.

Bindlish, R., and A. P. Barros, 2000: Disaggregation of rainfall for one-way coupling of atmospheric and hydrologic models in regions of complex terrain. *Global Planet. Change,* **25,** 111–132.

Bosilovich, M. G., Y. C. Sud, S. D. Schubert, and G. K. Walker, 2003: Numerical simulation of the large-scale North American monsoon water sources. *J. Geophys. Res.*, **108,** 8614, doi:10.1029/2002JD003095.

Brown, D. P., and A. C. Comrie, 2002: Spatial modeling of winter temperature and precipitation in Arizona and New Mexico, USA. *Climate Res.,* **22,** 115–128.

Carleton, A. M., 1986: Synoptic-dynamic character of "bursts" and "breaks" in the south-west U.S. summer precipitation singularity. *J. Climatol.,* **6,** 605–623.

Daly, C., R. P. Neilson, and D. L. Phillips, 1994: A statistical-topographic model for mapping climatological precipitation over mountain terrain. *J. Appl. Meteor.,* **33,** 140–158.

——, W. P. Gibson, G. H. Taylor, G. L. Johnson, and P. Pasteris, 2002: A knowledge-based approach to the statistical mapping of climate. *Climate Res.,* **22,** 99–113.

Deutsch, C. V., and A. G. Journel, 1998: *GSLIB—Geostatistical Software Library and User's Guide*. 2d ed. Oxford University Press, 369 pp.

Diaz, H. F., M. Grosjean, and L. Graumlich, 2003: Climate variability and change in high elevation regions: Past, present, and future. *Climate Change,* **59,** 1–4.

Drogue, G., J. Humbert, J. Deraisme, N. Mahr, and N. Freslon, 2002: A statistical-topographic model using an omnidirectional parameterization of the relief for mapping orographic rainfall. *Int. J. Climatol.,* **22,** 599–613.

EDAC, 1996: 60 meter elevation grid image for the state of New Mexico. Earth Data Analysis Center Albuquerque, NM, DEM map.

Fawcett, P. J., J. R. Stalker, and D. S. Gutzler, 2002: Multistage moisture transport into the interior of northern Mexico during the North American summer monsoon. *Geophys. Res. Lett.,* **29,** 2094, doi:10.1029/2002GL015693.

Goodrich, D. C., J. Faures, D. A. Woolhiser, L. J. Lane, and S. Sorooshian, 1995: Measurement and analysis of small-scale convective storm rainfall variability. *J. Hydrol.,* **173,** 283–308.

Goovaerts, P., 2000: Geostatistical approaches for incorporating elevation into the spatial interpolation of rainfall. *J. Hydrol.,* **228,** 113–129.

Hevesi, J. A., J. D. Istok, and A. L. Flint, 1992: Precipitation estimation in mountain terrain using multivariate geostatistics. Part I: Structure analysis. *J. Appl. Meteor.,* **31,** 661–676.

Higgins, R. W., K. C. Mo, and S. D. Schubert, 1996: The moisture budget of the central United States in spring as evaluated in the NCEP/NCAR and the NASA/DAO reanalyses. *Mon. Wea. Rev.,* **124,** 939–963.

——, Y. Yao, E. S. Yarosh, J. E. Janowiak, and K. C. Mo, 1997: Influence of the Great Plains low-level jet on summertime precipitation and moisture transport over the central United States. *J. Climate,* **10,** 481–507.

Hutchinson, P., 1973: The interaction of relief and synoptic situation on the distribution of storm rainfall in the vicinity of Dunedin. *N. Z. Geogr.,* **29,** 31–44.

Kyriakidis, P. C., J. Kim, and N. L. Miller, 2001: Geostatistical mapping of precipitation from rain gauge data using atmospheric and terrain characteristics. *J. Appl. Meteor.,* **40,** 1855–1877.

Michaud, J. D., B. A. Avine, and O. C. Penalba, 1995: Spatial and elevational variations of summer rainfall in the southwestern United States. *J. Appl. Meteor.,* **34,** 2689–2703.

Mock, C. J., 1996: Climatic controls and spatial variations of precipitation in the western United States. *J. Climate,* **9,** 1111–1125.

NOAA, cited 2004: Special feature: The North American Monsoon system. [Available online at http://www.srh.noaa.gov/abq/climate/Monthlyreports/July/nams.html.]

Oki, T., K. Musiake, and T. Koike, 1991: Spatial rainfall distribution at a storm event in mountainous regions, estimated by orography and wind direction. *Water Resour. Res.,* **27,** 359–369.

Phillips, D. L., J. Dolph, and D. Marks, 1992: A comparison of geostatistical procedures for spatial analysis of precipitation in mountainous terrain. *Agric. For. Meteor.,* **58,** 119–141.

Sellers, W. D., and R. H. Hill, 1974: *Arizona Climate 1931–1972*. 2d ed. University of Arizona Press, 616 pp.

Sheppard, P. R., A. C. Comrie, G. D. Packin, K. Angersbach, and J. K. Hughes, 2002: The climate of the US Southwest. *Climate Res.,* **21,** 219–238.

Sotillo, M. G., C. Ramis, R. Romero, S. Alonso, and V. Homar, 2003: Role of orography in the spatial distribution of precipitation over the Spanish Mediterranean zone. *Climate Res.,* **23,** 247–261.

Spatial Climate Analysis Service, cited 2003: Climatology normals (1971–2000). Oregon State University. [Available online at http://www.ocs.oregonstate.edu/prism/products/.]

Sturman, A., and H. Wanner, 2001: A comparative review of the weather and climate of the Southern Alps of New Zealand and the Europe Alps. *Mt. Res. Dev.,* **21,** 359–369.

Young, C. B., C. D. Peters-Lidard, A. Kruger, M. L. Baeck, B. R. Nelson, A. A. Bradley, and J. A. Smith, 1999: An evaluation of NEXRAD precipitation estimates in complex terrain. *J. Geophys. Res.,* **104** (D16), 19 691–19 703.

Woodhouse, C. A., and D. M. Meko, 1997: Number of winter precipitation days reconstructed from Southwestern tree rings. *J. Climate,* **10,** 2663–2669.